Automatic Multi-resolution Spatio-Frequency Analysis for Print Mottle Evaluation

Siddharth Khullar[1], Eli Saber[1], Sohail Dianat[1], Jeff Trask[2], Robert Lawton[2] and Mark Shaw[2]
1) Department of Electrical Engineering, Rochester Institute of Technology, Rochester, New York, USA.
2) Hewlett Packard Company, Boise, ID.

Abstract:

Evaluation of mottle is an area of on-going research in print quality assessment. We propose an unsupervised evaluation technique and a metric that measures mottle in a hard-copy laser print. The proposed algorithm uses a scanned image to quantify the low frequency variation or mottle in what is supposed to be a uniform field. 'Banding' and 'Streaking' effects are explicitly ignored and the proposed algorithm scales the test targets from "Flat print" (Good) to "Noisy print" (Bad) based on Mottle only. The evaluation procedure is modeled as feature computation in different combinations of spatial, frequency and wavelet domains. The algorithm's results are tested on a dataset of about 23 K only test targets out of which 13 were strictly for performance testing and results representing 10 targets are quantified in the paper against subjective rankings from ~30 Print Quality Experts (PQE) resulting in a ~ 91% correlation.

1. Introduction

Measurement of print quality is essential in many applications such as development of print-defect detection algorithms and photographic printing. It is imperative for print engines in use today to meet stable image quality requirements as evaluated by various metrics. The current marketplace demands the best image quality at competitive costs with minimum downtime. Hence, the ability for print engine vendors to efficiently achieve the highest levels of quality will ensure them a leadership role in the printing industry.

Ordinarily, these measurements are made by a Print Quality Expert (PQE) using various psychometric techniques. Unsupervised measurement of print quality is a topic widely being worked upon by many scientists in this field and has yielded impressive results. The characterization and evaluation of print mottle is an important step in assessment of print quality and is also a primary parameter of a hard copy print that we tackle in this paper.

Many evaluation models have been proposed for assessment of print quality in the past. Initial approaches include band-pass analysis, texture analysis, and measurement of specific perimeter and coefficient of variation. Johansson [1] proposed a method based upon the spatial wavelength analysis and named it as Band Pass Analysis (BPA). A modified coefficient of variation highlighting the effect of mean reflectance on print mottle was proposed by Fahlcrantz et al. [2]. The authors claim the method proposed in [1] earlier overestimates the mottle in dark prints but underestimates the lighter ones. Based on theoretical evidence and empirical testing, authors in [2] propose a square-root dependency of perceived luminance level on physical luminance level instead of the original cube-root relation in the CIELAB equation. Moving to evaluation of systematic print mottle, Fahlcrantz [3] proposed a model to evaluate variations that were systematic in nature. The model considered the variation between wavelengths of 0.25 and 16 mm and used a Contrast Sensitivity Function (CSF) of the HVS (Human Visual System) in form of a weighting vector to adjust variation in sensitivities at different frequencies. This model lacked the ability to perform a local analysis of printed area, and was also sensitive to half-tone screening defects due to its sensitivity to high frequencies.

All the above methods are also compared by Fahlcrantz et al. [4]. They conceptually examine and compare different techniques including ISO/IEC 13660 to postulate all aspects governing visual print-quality assessment and also question the need of a model-dependent ISO standard with emphasis laid upon whether ISO 13660 is a complete standard or not. ISO 13660 being based on density variations divides the evaluation model into two measurements – Graininess and Mottle, based on crude-band pass partitioning where higher frequencies correspond to the former and lower frequencies correspond to the latter, the partition threshold is set at 0.4 cycles/mm (~10 cycles/inch).

More recently proposed color mottle evaluation metric [5, 6] is based on prior work done in the grayscale domain. However, the evaluation of color mottle is done by assuming conditional independence of channel information. In this paper, we evaluate mottle in test targets printed using K component only in CMYK printers.

Techniques based on multi-scale and multi-resolution analysis have long been in existence in reference to print quality. Eid et al. [7] utilized a combination of the Discrete Wavelet Transform (DWT) and the ISO/IEC 13660. The results of this technique prove to be a lot better than those of ISO/IEC 13660. Another approach proposed by Donohue et al. [8] examines the wavelet analysis, exploiting its localized spatio-frequency properties for characterizing defects of limited spatial support.

In this paper, we propose a novel algorithm for automatic evaluation of mottle in what is ideally supposed to be a uniform print. We make use of a multi-resolution approach to generate a de-noised perceptual approximation from the input image and then process this image in the spatial and frequency domain separately, resulting in several features characterizing mottle. An effective outlier removal module facilitates the algorithm to provide with a more meaningful mottle number by removing the features which do not characterize the non-uniformity of test targets. A final metric value for total amount of mottle is obtained using the valid features and is known as the Spatio-Frequency Mottle Metric (SFMM).

The paper is organized as follows. Section 2 gives a description of various modules of the proposed algorithm. This is followed by a ranking module in Section 3 whereas Section 4 describes the Visual Evaluation Procedure (VEP) against which the algorithm's results are correlated. Results are shown in Section 5 and conclusions are drawn in Section 6.

2. Proposed Algorithm

An outline of the proposed algorithm primarily consisting of 3 modules is shown in Fig. 1. The first module (M1) is known as the pre-processing module and is responsible for preparing the input image for feature calculation. This module mainly performs the wavelet de-noising procedure on a cropped version of input image from the scanner. The second module, spatio-frequency parameter estimation (M2) handles feature computation in both, spatial and frequency domains and provides the third module (M3) with an a priori dataset to sort and remove outlier features. The third module consists of an Insignificant Feature Removal Stage (Outlier Removal) which is responsible for removing the Insignificant features from the feature set and give the value of the SFMM. Algorithm's performance evaluation is done by comparing ranks of SFMM against each target's visual scaling results, and a measure of performance is calculated in terms of correlation between the measured value and the visual scaling.

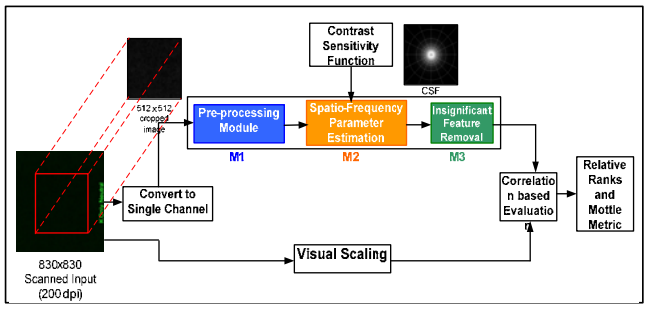

Figure 1: *Block diagram of the proposed SFMM Evaluation algorithm*

2.1 Pre-processing Module

Each test page consists of two targets - (1) K only and (2) Process Neutral, scanned at 200 dpi. The scanner used is HP Scanjet G4010 which has a six color lamp system. Each test target is acquired twice, once with all 6 lamps active and subsequently with two green lamps active. Note that, green lamp is the most sensitive to non-uniformities in luminance values, hence using it exclusively for K-only targets. This advantage of the scanner eliminates the need for calibration for luminance variations.

The input image acquired from the scanner has dimensions about 830x830 and is converted to grayscale Eqn. (1):

$$I_{gray} = 0.2989R + 0.5870G + 0.1140B \quad (1)$$

where I_{gray} is the final grayscale image and [R, G, B] are three channels of the TIFF file input from scanner. Note that the coefficient of green channel is greater than the coefficients of other two. The red and blue channels are included in the input image as they may contain variation information which could be lost on selecting only the green channel. The resultant grayscale image is cropped with respect to center of the original image as shown in Fig. 2 such that the features can be computed efficiently. Next, the image obtained here goes through the wavelet de-noising stage which comprises the most significant portion of this module.

Wavelets have long been used in image compression and signal de-noising. Wavelet basis functions are spatially localized and give information of both scale and frequency. Here, we use a similar technique described by Mangin [8] where the image is down-sampled using DWT analysis to 4 levels and all details (horizontal, vertical and diagonal) are completely removed. This leaves only the approximation at level 4 or what we strictly call, low frequency information. This approximation is then sent through a process of Wavelet synthesis using the same filter banks employed in the aforementioned analysis procedure. This yields final reduced-noise image or what is also known as the *'Perceptual Approximation'*. The filter banks used for Wavelet analysis/synthesis are the same as used in JPEG2000 compression standard.

The down-sampling process is done until 4 levels, because the peak of chosen CSF (explained in Section 2.3.1) occurs at a spatial frequency of 6.25 cycles/inch, this corresponds to a wavelength, λ = 0.16 inches or a scale of 32 pixels. Thus, as described above, all high frequency horizontal, vertical and diagonal details denoted as H, V and D respectively, are removed and a de-noised image of resolution 512x512 pixels is synthesized using the same filters (See Fig. 2).

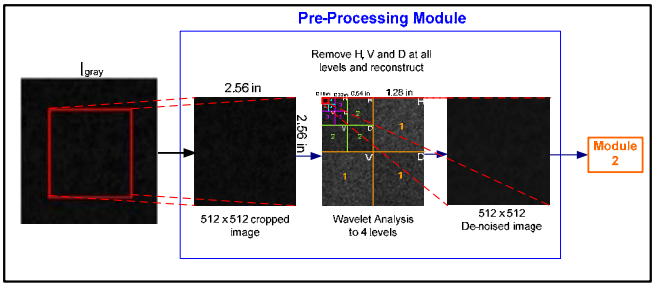

Figure 2*: Detailed block diagram pre-processing module (M1)*

2.2 Spatio-Frequency Parameter Estimation

The parameter estimation module comprises of 2 major sub-modules. One evaluates parameters (alternatively referred as features) strictly in the frequency domain, and the other computes features in the spatial domain. In Section 2.3.1, we explain the Contrast Sensitivity Function (CSF) followed by functions of the two sub-modules (2.3.2-2.3.3).

2.2.1 Contrast Sensitivity Function

Five CSF models as described in [10] were implemented for experimental purposes. The radial frequency axes for the CSF are implicitly generated by making use of the sampling theorem (See Figure 3).

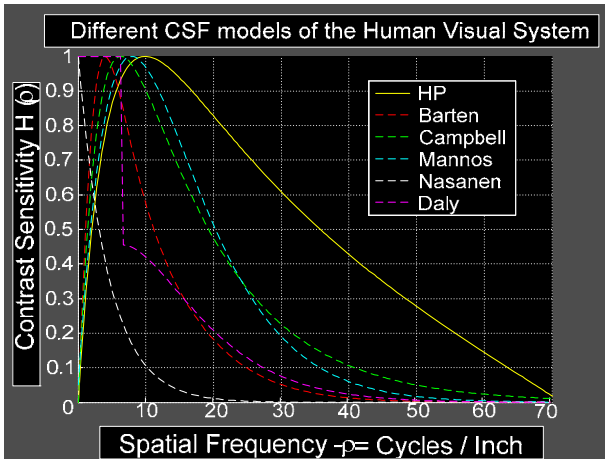

Figure 3: *Different 1-D CSF curves implemented originally in 2D for filtering.*

The size of the image and the scanning resolution (sampling frequency) are set at 512x512 pixels and 200 dpi respectively. Our purpose in using the CSF is to simulate the behavior of the HVS to compute one of the features in frequency domain.

2.2.2 Frequency Domain Analysis

As mentioned previously, the initial objective is to compute features that give a measure of variation across the test target.

A 2-D Fast Fourier Transform (FFT) of the 512 x 512 test image generated at the end of the pre-processing stage, is computed, and subsequently power spectrum (Squared Magnitude) is calculated. We subtract the mean of the image before taking the FFT for the purpose of normalization. The effects due to banding and streaking are also eliminated by setting the first row and column of the power spectrum to zero.

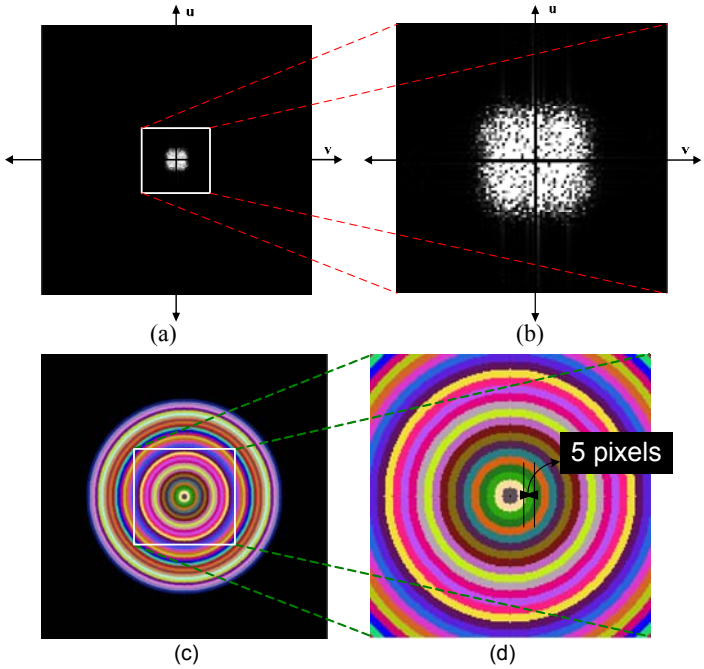

Figure 4: *(a) 2-D FFT (centered) of 'perceptual approximation'; (b) cropped version of (a) to re-iterate the absence of any high frequency content; (c) BRBM (5 pixels width) in image dimensions; (d) BRBM corresponding to low frequency content.*

These values can now be used to compute the following two features: 1) Ring Mottle (M_{rings}); 2) Spectral Entropy (E_{spec}). To compute M_{rings}, we make use of a technique known as 'radial filtering'. It can clearly be seen from Fig. 4 (a) – (b) that the power spectrum contains only low frequency content. To perform 'radial filtering', we define radial frequency bands as Binary Radial Band Maps (BRBMs) which are each multiplied with the power spectrum and subsequently pixel values are added providing energy in each band. BRBMs start from center with radial width of 5 pixels corresponding to the lowest radial frequency band. A pseudo-color representation of these BRBMs together is shown in Fig. 4 (c) – (d).

BRBMs are multiplied with the image, to demonstrate the phenomenon of frequency domain filtering, subsequently giving energy (measure of variation) in each band. Discrete power spectrum *P(u, v)* of an N x N image where *u* and *v* represent frequencies along X-direction and Y-direction respectively (see Fig.4), *P(u, v)* is multiplied point-by-point with the CSF described in section 2.2.1 resulting in a filtered signal that depicts the HVS response. The expression for uniformity in each band is given below:

$$U_i = \sum_{u=1}^{N}\sum_{v=1}^{N}[P(u,v)C(u,v)]H_i(u,v) \qquad (2)$$

where, *C(u, v)* is the 2-D Campbell's CSF (Fig. 3), $H_i(u, v)$ is BRBM of i^{th} frequency band (Fig. 4) and U_i gives the energy in the i^{th} frequency band. Consequently, the Ring Mottle (M_{rings}) is computed utilizing the aforementioned uniformity (U_i) in each band (Eqn. 2):

$$M_{rings} = \sum_{i=1}^{f_0}\left(U_i \big/ N\right) \qquad (3)$$

where, $f_0 = \sqrt{u^2 + v^2}$ cycles/inch and FFT Size, $N = 512$.

The next feature computed is Spectral Entropy (E_{spec}), using the probability distribution of the power spectrum *P(u, v)*. The following expression is used for computing E_{spec}:

$$E_{spec} = -\sum_{u=1}^{N}\sum_{v=1}^{N}\Pr(u,v)\ln\{\Pr(u,v)\} \qquad (4)$$

where, $\Pr(u,v) = P(u,v) \big/ \sum P(u,v)$ is the probability distribution of *P (u, v)*. When texture of the discrete power spectrum is more random, all probability values are significantly high, yielding large entropy values and vice-versa. This implies, a highly irregular pattern needs more information to be described, hence high entropy. Note that, spectral entropy is not calculated using the ring-shaped masks, but over the whole power spectrum (Fig. 4(a)).

2.3.3 Spatial Domain Analysis

The motive behind exploring the spatial domain is the flexibility provided by various statistical methodologies such as first and second order textural features using the co-occurrence (CO) matrices of size L x L (depending on the dynamic range of the image). CO matrices are calculated in 4 directions (0^o, 180^o, 90^o and -90^o) represented in Fig. 5 below and then cumulated together to give one CO matrix.

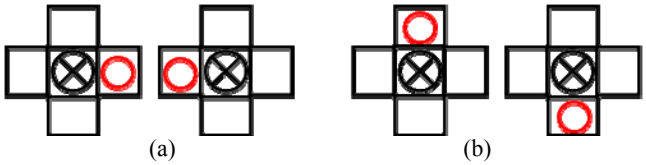

Figure 5*: Directional setting for Co-occurrence matrix (a) 0^o and 180^o; (b) 90^o and -90^o.*

After the final CO matrix (*Q(m, n)*) is obtained, a set of pre-selected features [11] is calculated: Angular Second Moment (ASM), Inverse Difference Moment (IDM), and Spatial Entropy (ENTR). The following three equations summarize the above mentioned features.

$$ASM = \sum_{m=0}^{L-1}\sum_{n=0}^{L-1}[Q(m,n)]^2 \qquad (5)$$

$$IDM = \sum_{m=0}^{L-1}\sum_{n=0}^{L-1}Q(m,n)\left[1+(m-n)^2\right] \qquad (6)$$

$$ENTR = -\sum_{m=0}^{L-1}\sum_{n=0}^{L-1} Q(m,n)\log_2[Q(m,n)] \quad (7)$$

ASM corresponds to amount of orderliness in the target. If the texture is extremely random or the variation is high, the value of ASM is low and vice versa. Same is the case for IDM. Hence, these values are sorted in descending order to be in accordance with the ranking algorithm which works on the principle of lowest to highest (Best to Worst). IDM has smaller numbers for images with high contrast, larger numbers for images with low contrast.

The next spatial feature included is based on the one described by Rosenberger in [12], known as the Stochastic Spatial Frequency Distribution Analysis (SFDA). The advantage of adding this feature is that it is based on local variation information of the test target. Also, originally this feature is intended to compute the amount of graininess in the target, but we modified it to provide us with a measure of mottle in the target. A formula different from [12] is used in our metric.

In any digital image which consists of low frequency gray level variation, the SFDA algorithm proposed by Rosenberger in [12] measures the two dimensional rate of change in luminance values and transitions between light and dark throughout the image. Many parameters affect our visual system as described in [12]. To corroborate this fact, the author states - "The human visual system operates in a three dimensional environment (Subjective Analysis setup) composed of the luminance intensities governed by parameters like length and height of the viewing area relative to the observer's visual system". SFDA extracts square contiguous target areas of the same pixel dimensions in an iterative fashion, as shown in Fig. 6 below:

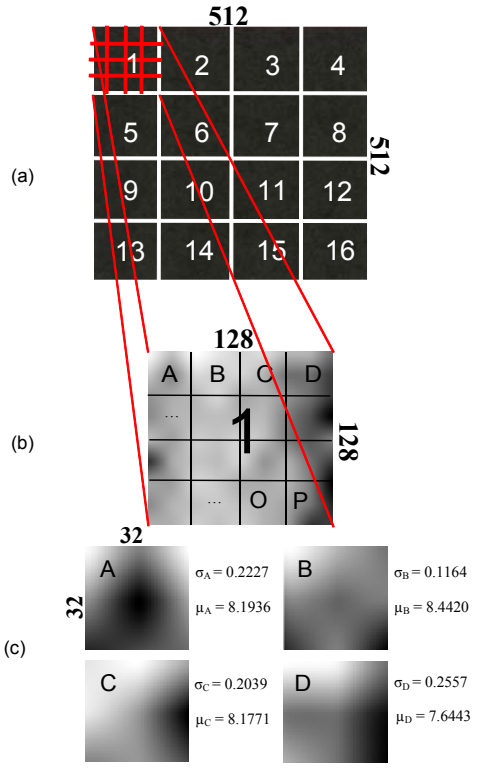

***Figure 6**: Spatial Distribution: (a) A typical target size (512x512) composed of 16 128x128 targets.(b) Spatial distribution of sub-target no. 1 shown in (a), 4x4 grid shown on large 128x128 target; (c) expanded view of first 4 sub-targets in (b).*

A rather different metric than SFDA is used here, but is not named differently. The main test target is divided into 16 tiles of size 128x128 pixels (Fig. 6(a)-(b)). These bigger tiles are labeled with index i = [1, 2,…..,16]. Each i^{th} tile is further sub-divided into 16 tiles each of size 32 x 32 pixels (Fig. 6(c)). These smaller tiles are labeled as [A, B, ……. , O, P]. Now, the mean and standard deviations for all 32x32 targets are calculated. This yields 2 vectors, one is the standard deviation vector α_i = [σ_A, σ_B, σ_C, σ_D, σ_E , ……, σ_P] and other is the mean vector β_i = [μ_A, μ_B, μ_C, μ_D, μ_E, ……., μ_P], i =[1,2,3…,16] representing each 128x128 tile.

We compute 3 attributes using the above two vectors to facilitate the final computation of mottle. These are known as μ_i (Mean of α_i), σ_i (standard deviation of α_i) and $\mu_{\beta i}$ (Mean of β_i). The target mean, $\mu_{\beta i}$ is a good indicator of diversity of visual intensities or local area contrasts. Next we compute, what is called the Local Mottle for each 128x128 sub-target. The expression for it is given as:

$$M_{(i),Local} = \mu_i \sigma_i \mu_{\beta,i} \quad (8)$$

where, $M_{(i),\,Local}$ represents the mottle for each 128x128 tile. This process, when carried out for all 16 tiles, gives us a vector which consists of local mottle values. This expression is different from the one proposed by [12] in the sense that original SFDA uses standard deviation of β_i rather than the mean. The reason behind this change is that the mean and standard deviation of α_i collectively provide us with the degree of variation amongst α_i consequently giving a measure of uniformity in the small 128x128 sub-targets and the mean $\mu_{\beta i}$ acts as a local scaling factor for that particular sub-target. These 3 factors, when multiplied together provide a good local variation estimate. Final SFDA mottle value is expressed as a product of standard deviation of $M_{(i),\,Local}$ and its mean.

$$Mottle_{SFDA} = \mu_{Mi}\sigma_{Mi} \quad (9)$$

The proposed change in the existing SFDA algorithm resulted in a better co-relation with the subjective rankings.
The parameters given by Eqns. (3) – (7) and (9) give the 6 features that comprise the final value of SFMM.

3. Ranking Algorithm

After obtaining all features (attributes) from Module 2 for all 10 test targets, the data is organized in form of vectors. These vectors are further normalized with respect to the local maximum value. This is done to limit the maximum SFMM value to number of features. Next, the normalized parameters are obtained in form of a matrix of size M x N where M equals number of test targets (10) and N is the number of features (6) known as the Feature Value Matrix (FVM). A tabulated version of FVM for 10 targets in consideration is shown in Table 1.

The a priori ranking is obtained by arranging most of the features in ascending order, though this is not the case with ASM and IDM, which are ranked in descending order to maintain the consistency with other 4 features (Table 1). In any feature vector, rank 1 corresponds to the "Best sample" and 10 correspond to the "Worst Sample". Rankings can be compared along columns, each target contains a majority rank which has the highest frequency of occurrence and is known as the Cumulative Rank (CR).

3.1 Insignificant Feature Removal Stage

This part of the algorithm removes the insignificant features using a maximum correlation based criterion between each feature rank and CR. In the ranking process, n test targets are ranked in r

different rankings according to 6 features. The mode rank i.e. the number with most occurrences for a test target is assigned as its CR.

For example, if 4 features rank a target as '1' and rest two features rank it 5 and 6, then these two features would be considered as outliers. To find and eliminate these outliers, we developed a vote-based outlier removal algorithm. Duplicate rankings do not make a difference in the final results.

Insignificant Features and Correlation Information							
Test Target	Ring Mottl	Spec. Entropy	ASM (Desc)	IDM (Desc)	Entropy	SFDA	CR
1	1	5	3	1	4	1	1
2	2	10	1	4	1	5	1
3	5	1	4	5	3	3	3
4	7	7	7	3	7	7	7
5	3	8	2	7	2	2	2
6	6	3	6	6	6	6	6
7	9	4	9	9	9	9	9
8	4	9	5	2	5	4	5
9	8	2	8	8	8	8	8
10	10	6	10	10	10	10	10
CORR	0.97	-0.31	0.98	0.66	0.96	0.92	1

Table 1: Feature Rank Matrix for 10 test targets with Cumulative Ranks and Outlier information ('1' = Least Mottle; …… '10' = Most Mottle).

The last row in Table 1 gives the correlation between CR and corresponding feature ranks. The criterion for removing outliers is a correlation threshold. If the correlation between CR (also known as a priori ranks) and rank of corresponding feature is less than 80%, it is declared as an outlier. This value is fixed at 80%, fulfilling the level of accuracy we require. The columns for outlying features are set to 0 in the FVM (See Table 1).

4. Visual Evaluation Procedure (VEP)

There have been many weighted sum based algorithms proposed to find a many-to-one mappings of psychometric ranking from several human visual observers. A similar technique is used here to find the cumulative ranking which is described in [13].

Given 10 test targets, these are ranked in r different rankings according to m observers. First, a sum of rank values is computed using the following expression:

$$S_i = \sum_{k=1}^{N} f_{ik} R_k \qquad (10)$$

where i represents the i^{th} image and varies from 1 to 10. The index k gives the rank and also varies from 1 to 10. The term f_{ik} represents the number of observers that give ith image a rank k. The term R_k is a vector in the reverse order to k and is given by $R_k = n - k + 1$. Finally, these values of S_i are arranged in descending order and the indices corresponding to this order are given as ranks to the images corresponding to i. A way of combining all subjective rankings for comparison with the algorithm using correlation statistics has been presented here. The method explained above is applied only to data obtained from visual scaling experiments done at Rochester Institute of Technology by laymen observers. The final algorithm rankings have been compared against the ones obtained at the HP facility in Boise, ID by about 30 Print Quality Experts (Fig. 7).The next section summarizes the results in detail along with the final rankings for each sample followed by the conclusions.

5. Results

The SFMM results were compared against those obtained from the VEP to analyze its overall performance. We compared the SFMM against the visual rankings obtained previously, on the basis of correlation. The graphical representation is shown in Fig. 13 followed by a tabulated summary of SFMM, Visual Evaluation Procedure and their correlation in Table 5.

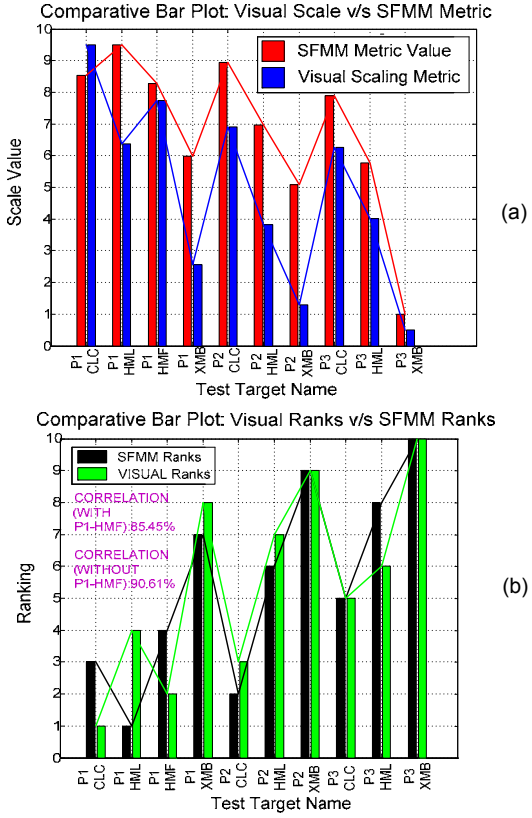

Figure 7: *Correlation curves between (a) SFMM Metric and VEP metric, (b) SFMM ranks and VEP ranks (with Correlation details).*

In Fig. 7(a), the two SFMM is mapped on a scale of 10 by a simple linear transformation and is plotted against the VEP scale value (Table 2). In Fig. 7(b), a separated distribution of ranks from SFMM and VEP is shown along with the correlation. One of the ambiguities where one of the samples - "P1-Hammer Mill Fore" was given a rank 4 on the uniformity scale by the observers and SFMM ranked it to be the best sample, lowers the correlation considerably from 91% to 85%.

Test Target	Printer	Media	SFMM	Rank	VEP (HP)	Visual Rank
1	P1	Canon Color Laser	0.989	3	9.5	1
2	P1	Hammermill Fore	0.5979	1	6.36	4
3	P1	Hammermill Laser	1.0907	4	7.75	2
4	P1	Xerox Bus. 4200	2.0018	7	2.56	8
5	P2	Canon Color Laser	0.8259	2	6.91	3
6	P2	Hammermill Laser	1.6118	6	3.82	7
7	P2	Xerox Bus. 4200	2.3665	9	1.29	9
8	P3	Canon Color Laser	1.2449	5	6.26	5
9	P3	Hammermill Laser	2.0912	8	4.02	6
10	P3	Xerox Bus. 4200	4	10	0.5	10

Table 2: Result Summary with SFMM value and relative rank alongside the visual rankings

The reason for this ambiguity will be clear once the second pass of the visual scaling is carried again and when we further add features to the algorithm. This would be explained in the next version of the metric as a part of future work. We tested another 13 test targets with varying amount of mottle, different optical density, printed using 4 different printers and 4 different media. The algorithm gave excellent results with correlations up to 90%. That data is out of the scope of this paper and hence not provided here.

In Table 2, a sorted list of data is given according to the scanning sequence of targets. In total 3 printers were used in the generating the test targets – (1) "P1"; (2) "P2" and (3) "P3". Further, four different media were used to print 10 test targets. These media were – (1) Canon Color Laser; (2) Hammermill Fore; (3) Hammermill Laser; (4) Xerox Business Multipurpose 4200.

The printer type and media type are mentioned for each test target in the table. Note that the maximum SFMM (~4) value does not exceed the number of features. This was done to maintain consistency and signify the number of features finally included in evaluation of SFMM.

6. Conclusions and Future Work

In this paper, we propose a methodology of evaluating only low frequency content using a novel combination of Spatial, Frequency and Wavelet domain and also device a metric that provides a fairly accurate estimate of mottle in a given test target. The proposed metric - SFMM undoubtedly agrees well (correlation ~ 91%) with the visual scaling results for these nine out of ten test targets.

Few other observations were also made, such as permanent elimination of a few features and future trials with some other additional features based on spatial domain evaluation. The Coefficient of Variation (COV) for all test targets highly un-correlated with other features' rankings and hence can be removed permanently from the metric. Also, the Spectral Entropy (E_{spec}) resulted in a negative correlation leading us to consider its inclusion in the metric even for a priori calculation in the next version of the algorithm. These features effect the computation of CR as they are considered while the maximum vote is determined.

The next step is to develop a method for evaluating the test targets subjectively here at RIT which will be a pair-wise comparison given a constant set of luminance conditions and large number of casual observers. Expert evaluations would also be obtained and compared alongside the layman rankings against the algorithm results.

Concerning the advantages of this new model over previous models available, the most important contribution is the introduction of a combinative analysis using spatial and frequency features with prior pre-processing using wavelets. To our knowledge, no attempt has been made to combine these features together and make a single model for evaluation of print mottle. All our results do in fact indicate that this rather straightforward method works surprisingly well in many circumstances.

The second important advantage is of the scanner being used. The scanned image, being acquired using the six color lamp system and a customized routine adds to the algorithms robustness and eliminates any questions related to calibration and acquisition errors.

This work is proposed to be extended another level of complexity. Evaluation of print mottle in real life images is an area which still remains unexplored. Any such algorithm has, to our knowledge, not yet been published or developed. Currently, the proposed algorithm is compatible with only flat uniform images. Real life images consisting of regions with varying levels of optical density and uniformity need to be handled and evaluated differently. This is something that the authors intend to propose in their next work based on the current work.

References

1. P. Å. Johansson, "Print mottle evaluation by band-pass image analysis," *Advances in Printing Science and Technology*, Vol. 22, Pentech Press, London, pp. 403, 1993.
2. C-M. Fahlcrantz, P. Å. Johansson and P. Åslund, "The influence of mean reflectance on perceived print mottle," *Journal of Imaging Science & Technology,* Vol. 47, pp 54-59, 2002.
3. C-M. Fahlcrantz, "Evaluating Systematic Print Mottle," *Journal of Graphics Technology,* Vol. 1, Issue 2, pp 19-28, 2003.
4. C-M. Fahlcrantz and P. Å. Johansson, "A comparison of different print mottle evaluation models," *TAGA Proceedings,* San Antonio, 2004.
5. C-M. Fahlcrantz and J. Christoffersson, "Print mottle evaluation – An integrated approach," *International conference on Printing Technology,* St. Petersburg, Russia, 2006.
6. C-M. Fahlcrantz and K. Sokolowski, "Evaluating color print mottle", *33rd IARIGAI Research Conference,* Leipzig, Germany, 2006.
7. A.H. Eid, B.E. Cooper and E.E. Ripptoe, "Characterization of mottle and low frequency print defects," *Proceedings of the SPIE,* Vol. 6808, pp. 680809-680809-12, 2008.
8. K. Donohue, C. Cui, and M.V. Venkatesh, "Wavelet analysis of print defects," *Proc. of IS&T's 2002 PICS Conference,* pp. 42-47, Portland, OR, 2002.
9. P.J. Mangin and M. Dube, "Fundamental questions on print quality", *Proc. of IS&T's Electronic Imaging,* Vol. 6059, pp 605901-605901-12, 2006.
10. S.H. Kim and J.P. Allebach, "Impact of HVS Models on Model-based Halftoning", *IEEE Transcations on Image Processing,* Vol. 11, Issue 3, pp. 258-269, 2002.
11. S. Theodoridis and K. Koutroumbas, "Pattern Recognition", *Academic Press, Third Edition, pp 331-334,* 2006.
12. R. Rosenberger and D. Clark, "Stochastic Frequency Distribution Analysis as applied to inkjet print mottle measurement," *Proc. of IS&T's 17th Non-Impact Printing Conference,* pp-808-812, Fort Lauderdale, FL, 2001.
13. N. Abbadeni, D. Ziou and S. Wang, "Autocovariance-based perceptual textural features corresponding to human visual perception", *Proc. of the 15th IAPR/IEEE Intl. Conference on Pattern Recognition*, pp 3913-3916, Barcelona, Spain, 2000.

Author(s) Biography

Siddharth Khullar *is pursuing a PhD degree in Imaging Science from Rochester Institute of Technology, NY. He completed his MS degree in Electrical Engineering from RIT, NY and his B. Tech. (EE) from Indraprastha University, Delhi, India. His interests include print quality assessment, image understanding, image and video segmentation, data fusion, functional MRI imaging analysis techniques and Wavelet image processing.*

Eli Saber *is an Associate Professor in the Electrical Engineering Department and Chester F. Carlson Center for Imaging Science at the Rochester Institute of Technology, New York, USA. His interests include image processing, Image & Video segmentation, Print Engine development and print quality assessment.*

Sohail Dianat *is a Professor in the Electrical Engineering Department and Chester F. Carlson Center for Imaging Science at the Rochester Institute of Technology, New York, USA. His interests include, communication systems, wireless networks, color image processing and control systems.*